



Mechanics of mouse blastocyst hatching revealed by a hydrogel-based microdeformation assay

Karolis Leonavicius^{a,1}, Christophe Royer^a, Chris Preece^b, Benjamin Davies^b, John S. Biggins^c, and Shankar Srinivas^{a,2}

^aDepartment of Physiology, Anatomy and Genetics, University of Oxford, Oxford OX1 3QX, United Kingdom; ^bWellcome Centre for Human Genetics, University of Oxford, Oxford OX3 7BN, United Kingdom; and ^cDepartment of Engineering, University of Cambridge, CB2 1PZ Cambridge, United Kingdom

Edited by Janet Rossant, Hospital for Sick Children, University of Toronto, Toronto, ON, Canada, and approved August 15, 2018 (received for review November 15, 2017)

Mammalian embryos are surrounded by an acellular shell, the zona pellucida. Hatching out of the zona is crucial for implantation and continued development of the embryo. Clinically, problems in hatching can contribute to failure in assisted reproductive intervention. Although hatching is fundamentally a mechanical process, due to limitations in methodology most studies focus on its biochemical properties. To understand the role of mechanical forces in hatching, we developed a hydrogel deformation-based method and analytical approach for measuring pressure in cyst-like tissues. Using this approach, we found that, in cultured blastocysts, pressure increased linearly, with intermittent falls. Inhibition of Na/K-ATPase led to a dosage-dependent reduction in blastocyst cavity pressure, consistent with its requirement for cavity formation. Reducing blastocyst pressure reduced the probability of hatching, highlighting the importance of mechanical forces in hatching. These measurements allowed us to infer details of microphysiology such as osmolarity, ion and water transport kinetics across the trophoctoderm, and zona stiffness, allowing us to model the embryo as a thin-shell pressure vessel. We applied this technique to test whether cryopreservation, a process commonly used in assisted reproductive technology (ART), leads to alteration of the embryo and found that thawed embryos generated significantly lower pressure than fresh embryos, a previously unknown effect of cryopreservation. We show that reduced pressure is linked to delayed hatching. Our approach can be used to optimize in vitro fertilization (IVF) using precise measurement of embryo microphysiology. It is also applicable to other biological systems involving cavity formation, providing an approach for measuring forces in diverse contexts.

mammalian embryo hatching | embryo cryopreservation | pressure measurement | hydrogel deformation | mouse blastocyst

Blastocyst formation underpins the foundation of early mammalian development, occurring before embryo implantation into the uterus. During this process, the embryo creates a pressurized cavity within it and eventually breaks out of the protective acellular outer layer, the zona pellucida. Without hatching from the zona pellucida, embryos are unable to implant into the uterus, which therefore represents a stumbling block for in vitro fertilization (IVF) technologies (1). In addition to driving molecular changes to the trophoblast cells and the uterus (2), the timing of embryo hatching is also important, with early hatching resulting in ectopic pregnancies (3) and late hatching causing the window of receptivity to be missed (4). To date, the process has been difficult to study from the mechanobiology perspective due to the lack of suitable tools for imposing and characterizing deformations in 3D tissues. Moreover, embryo assessment is a crucial step during IVF procedures, particularly for evaluating the quality of cryopreserved embryos that have been thawed (5). However, existing methods rely on qualitative scoring, and a well-characterized quantitative methodology could provide more reliable predictive accuracy.

Previous studies have calculated tissue forces by directly observing the deformation of structures of known stiffness, for example by incorporating deformable oil droplets into developing tissues to

measure the anisotropic (shear) stress (6), or by culturing a layer of cells atop a 2D array of bendable hydrogel pillars (7) to measure traction. Atomic force microscopy has also been used to measure local mechanical properties of individual blastocyst cells (8) and the hydrogel shell (9–12). However, integrating the information into a systematic model has proven difficult due to a lack of embryonic force measurements. It is understood how embryonic tissue would respond to forces, but it is unknown what the forces are.

Mammalian preimplantation embryos have been intensely studied from the molecular biology perspective. These studies revealed much detail about the genetic regulation of cell fate decisions (13, 14) and the molecular mechanism of blastocyst cavity development. It has been shown that cavity expansion is driven by active ion transport (15), mediated by Na/K-ATPases in the outer epithelial cell layer sealed by tight junctions (16, 17). Increasing internal osmolarity then results in water transport along the osmotic gradient, which is mediated by aquaporin water channels (18, 19). These components act together to create the system responsible for internal pressurization of the cavity and eventual embryo hatching from its outer shell. The zona pellucida is composed of several glycoproteins, which form an elastic hydrogel layer around the embryo. The width of this layer decreases during embryo expansion as a precursor to hatching, partly in mechanical response to the tangential stretching imposed by the embryo's increasing volume,

Significance

Blastocyst hatching is crucial for implantation of mammalian embryos and a common failure point during in vitro fertilization (IVF). We have little knowledge of the mechanical basis whereby an embryo hatches out of the zona pellucida. We have developed a technique to measure blastocyst pressure, allowing us to quantify physiological parameters and providing additional measures of efficiency in IVF optimization. We find that mechanical stretching of the zona by the blastocyst is essential for efficient hatching. Cryopreservation and thawing of embryos is common during IVF. Our technique reveals significant differences in microphysiology between fresh and thawed embryos. Our experimental and associated mathematical techniques are also applicable to other biological systems involving cavity formation, providing an approach for measuring forces in diverse contexts.

Author contributions: K.L., C.R., and S.S. designed research; K.L., C.R., and C.P. performed research; C.P., B.D., and J.S.B. contributed new reagents/analytic tools; K.L., C.R., J.S.B., and S.S. analyzed data; and K.L., C.R., J.S.B., and S.S. wrote the paper.

The authors declare no conflict of interest.

This article is a PNAS Direct Submission.

This open access article is distributed under [Creative Commons Attribution-NonCommercial-NoDerivatives License 4.0 \(CC BY-NC-ND\)](https://creativecommons.org/licenses/by-nc-nd/4.0/).

¹Present address: Institute of Biotechnology, Vilnius University, Vilnius 10257, Lithuania.

²To whom correspondence should be addressed. Email: shankar.srinivas@dpag.ox.ac.uk.

This article contains supporting information online at www.pnas.org/lookup/suppl/doi:10.1073/pnas.1719930115/-DCSupplemental.

Published online September 19, 2018.

and partly due to the action of degrading enzymes (20–22). Although both mechanical and enzymatic factors have been suggested to be important, making a distinction between them has proven difficult due to the lack of experimental techniques.

Here, we therefore extend the idea of measuring mechanical forces using deformable media and develop an approach focused on confining embryos in hydrogels. This allows us to measure not only the pressure but also the dynamics of other important underlying processes, such as ion and water transport, and quantify the mechanical components of the hatching process. We use this approach to characterize the microphysiology of embryos and discover previously unknown blastocyst cavity pressure differences between freshly collected embryos and embryos thawed after cryopreservation.

Results and Discussion

Relating Hydrogel Deformation and Tissue Pressure. Developing E3.5 mouse embryos were embedded in microfabricated cylindrical cavities within hydrogels of known Young's modulus (E). Optical bright-field microscopy (Fig. 1A and [Movies S1](#) and [S2](#))

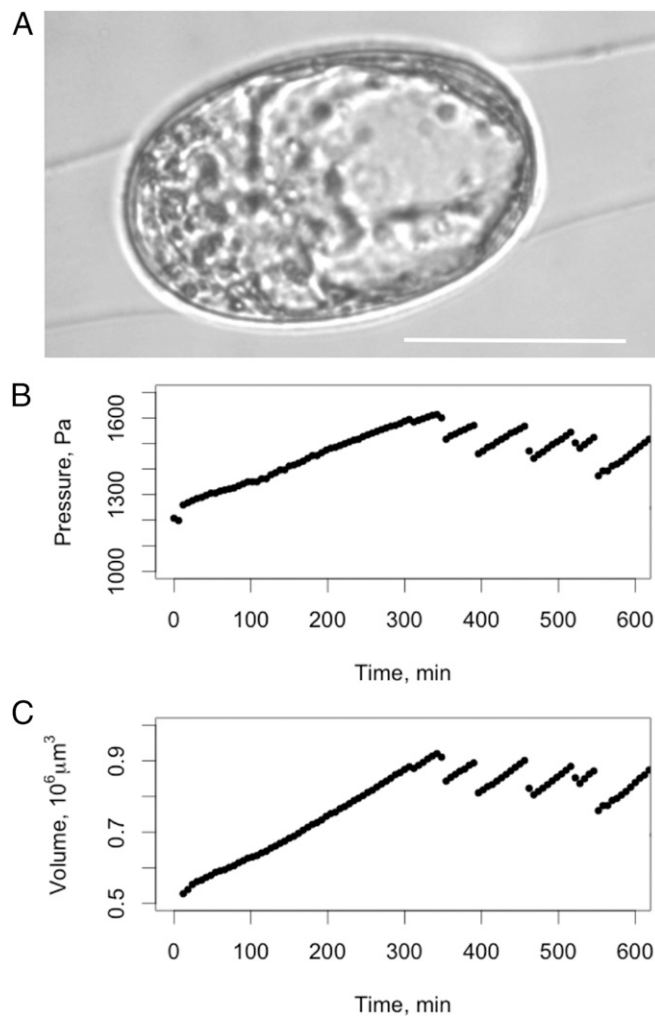


Fig. 1. Summary of embryo development in hydrogel cavities. Pressures in developing embryos were measured by using deformable hydrogels ([Movies S1](#) and [S2](#)) (A). The embryos were cultured from early cavity stage ~ 3.5 d after fertilization in KSOMaa Evolve media of osmolarity of 0.252 Osm. (Scale bar: 50 μm .) The elastic hydrogel made it possible to calculate the pressure (B), which was generated during volumetric expansion (C). The time lapse was taken over a period of 2 h with a resolution of 6 min.

was then used to measure channel dilation by the embryo from a (undeformed) to $a + h$ (maximum dilated radius; [SI Appendix, Fig. S1A](#)). A simple elastic model of the channel then allowed us to calculate the pressure exerted and hence the pressure P within the embryo as follows (Eq. 1: Calculating pressure exerted upon the hydrogel):

$$P = \frac{E}{6} \left(1 + 2 \ln(\tilde{R}) - \frac{1}{\tilde{R}^2} \right), \tilde{R} = \frac{a+h}{a}. \quad [1]$$

Our elastic model is exact for a channel dilated evenly from a to $a + h$ and remains a good approximation if h varies slowly along the channel. To confirm the validity of Eq. 1 in the experimental regime, we replaced embryos with oil droplets of known surface tension and hence known internal pressure, and confirmed that the model correctly reproduces droplet pressure ([SI Appendix, Fig. S1B](#)). Details of the elasticity calculation and droplet verification are in [Materials and Methods](#).

To test whether culturing embryos within the hydrogel impairs viability, we analyzed the number of inner cell mass and trophoblast (TE) cells, as well as the number of fragmented nuclei. Across various sets of experimental conditions, we found no significant differences between embryos cultured within hydrogels and control unconfined embryos, suggesting that our method was not harmful ([SI Appendix, Fig. S1 C–E](#)).

The Effects of Embryo Compression. Embryo compression itself is likely to generate some additional internal pressure based on elongating an embryo from the spherical shape. This requires the zona pellucida to stretch, which is an additional source of pressure. Therefore, internal embryo pressure is the sum of measured pressure acting on the hydrogel and the added pressure due to deformation from spherical to elongated shape. To estimate the pressure originating solely from the deformation, we consider that, on average, embryos increase pressure with increasing surface area at the rate of 0.03 Pa/ μm^2 . This can be estimated by tracking embryo area and pressure increases with time. It can also be estimated that compression results in surface area increase of less than 3,000 μm^2 , which indicates that internal pressure may be higher than measured by as much as 90 Pa. Since this is below the measurement error of 150 Pa, we can assume that pressure exerted on the hydrogel represents the internal embryo pressure. Also, the measurement error of 150 Pa made it impossible to measure zona pellucida free and hatched embryos, which could no longer significantly deform the hydrogel ([SI Appendix, Fig. S2](#)). Intact outer shell was required for generating a significant, measurable pressure.

Microphysiology of Blastocyst Cavity Development. To build a mathematical model for embryo hatching, it is crucial to look at the details of how all of the different components of the system create a pressurized cavity. By measuring blastocyst pressure and volume dynamics (Fig. 1B and C), we could see that pressure and volume rises were linear over the course of development, but interrupted by sudden drops, which likely corresponded to TE cell divisions or epithelial cell junction cycling ([SI Appendix, Fig. S3](#)). Overall, developing mouse blastocyst-stage embryos generated pressures of around 1.4 kPa and had an average volume of $0.66 \times 10^6 \mu\text{m}^3$ (Fig. 2A and B). These pressure and volume measurements allowed us to derive other important physiological parameters, such as blastocyst osmolarity using the van't Hoff (ideal gas) law (Eq. 2), where R is the ideal gas constant, V is cavity volume, and c_{media} is 0.252 Osm:

$$P = \Delta c RT = (c_{\text{cavity}} - c_{\text{media}}) RT. \quad [2]$$

This leads to the conclusion that typical pressurized embryo cavities have $\Delta c \sim 0.8$ mOsm of additional electrolytes. Furthermore, by

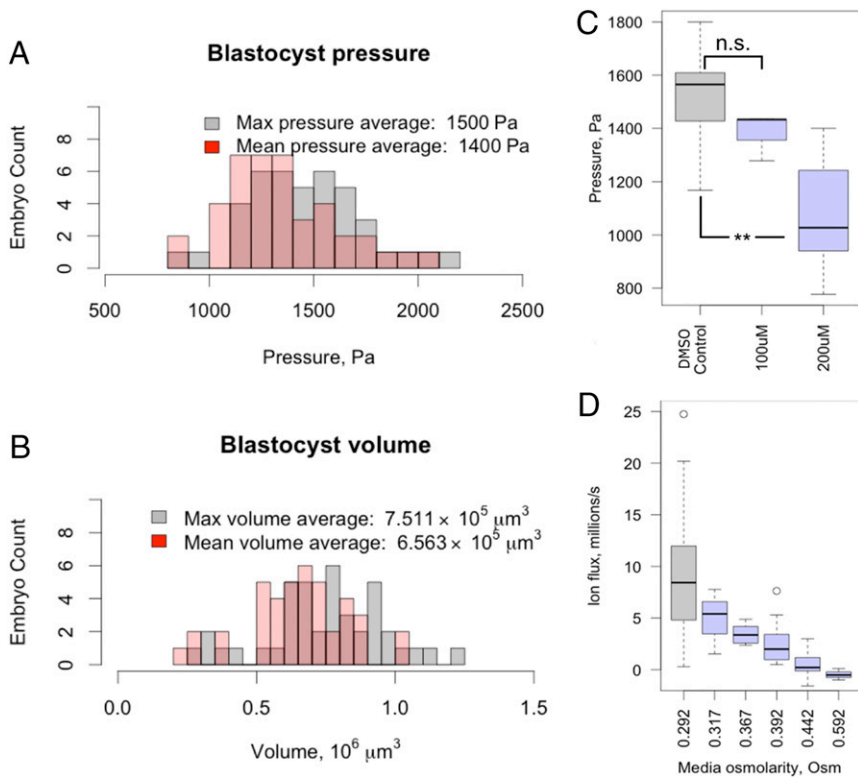


Fig. 2. Blastocyst pressure and volume measurements. (A) Pressure distribution in developing mouse embryos ($n = 41$). The small difference between the mean and maxima reflects the fact that embryos spend most of the time close to their maximal pressure. (B) Volume distribution in mouse embryos ($n = 41$). The average values were generated by measuring the maximum and mean pressures each embryo generates during development and then averaging these values over the normally developing embryos used for the experiments. (C) The generated pressure could be disrupted by using a Na/K-ATPase inhibitor ouabain. Embryos responded in a dose-dependent manner, which highlighted the importance of ion transport for blastocyst cavity expansion. The 100 and 200 μM inhibitor concentrations were achieved by diluting a 100 mg/mL DMSO stock; controls contained an equivalent amount of DMSO. At least seven embryos in each condition; P values are represented by the following: n.s., not significant; **, <0.01 . (D) Increasing media osmolarity reduces blastocyst cavity pressure because of the reduced ion influx into the cavity. The figure demonstrates that the rate of ion transport across the TE layer was dependent on the osmolarity balance between the outside and inside of the blastocyst cavity. At least five embryos were used per condition.

taking the time derivative of the above equation, and recalling that the total number of ions in the embryo is related to the ion concentration by $N_{\text{ions}} = c_{\text{cavity}} V N_A$, we can calculate the rate of ion transport into the embryo as shown in Eq. 3:

$$\frac{dN_{\text{ions}}}{dt} = \frac{1}{k_B T} \left(\frac{dP}{dt} * V(t) + \frac{dV}{dt} * P(t) \right) + N_A * \frac{dV}{dt} * c_{\text{media}} \quad [3]$$

Using estimates of P , V , and their rates of change gathered from Fig. 1, we conclude that, on average, every transported ion produced a $2.02 \times 10^{-6} \mu\text{m}^3$ volume increase and there were 10.1 million ions transported every second during cavity inflation. This would correspond to transport of a solution containing 0.80 mOsm of additional electrolytes, or 0.40 mM if the solution was NaCl. The low osmolarity value is consistent with previously published values obtained using different techniques (23).

The rate of pressure and osmolarity change also makes it possible to estimate the ion flux and the number of involved Na/K-ATPases. From previous studies (15), it is known that the ion gradient is primarily generated by the activity of Na/K-ATPase enzymes, which use energy to transport ions across an ion gradient. To verify that pressure generation was also actively driven, we used ouabain to inhibit ion transport (Fig. 2C), which indeed resulted in reduced cavity pressure in a dose-dependent manner. Additionally, ion transport was also found to be dependent on media osmolarity, which indicates that the process is actively regulated (Fig. 2D).

To estimate the number of Na/K-ATPases present on the trophoblast cells, we used published data reporting ATPase turnover rates. They have been calculated from radioactivity measurements and reported for every Na/K-ATPase to be around 3,600/min (Na^+) (24), 3,000/min (K^+ , Rb^+) (25), and 2,000/min (ATP) (26). Since every ATP molecule results in transfer of two K^+ ions into the cells and three Na^+ outside, the average rate for Na^+ transport could be estimated to be around 4,700/min. Since the dominant counterion in the media is Cl^- , sodium efflux can be estimated to be responsible for one-half of

the osmolyte flux, or $3.3 \times 10^8/\text{min}$. Using confocal imaging, we have estimated experimental embryos to contain 60 cells on average, 42 of which belong to the TE layer (SI Appendix, Fig. S1 C–E), which would result in ion flux per cell of $7.8 \times 10^6/\text{min}$, estimating 1.7×10^3 active ion transporters per cell. In addition to estimating the average number of active Na/K-ATPases operating in TE cells, we also looked at how embryos responded to rapid changes in osmolarity, which revealed water transfer kinetics reaching rates of $400 \mu\text{m}^3/\text{s}$, as 252 mOsm of sucrose was added to embryos developing in channels (SI Appendix, Fig. S4 A and B). Water flux during transient response is over 20 times the normal water transport rates seen during normal development (Table 1), suggesting that cavity expansion is limited and regulated by the rate of ion rather than water transport.

Mechanical Model of Zona Pellucida. Although liquid inflow and sealed epithelial layer are the prerequisites for cavity formation, pressure ultimately arises due to the constricting nature of the external polysaccharide shell zona pellucida. Since shell thickness can be measured by bright-field microscopy to be less than 1/10 of the embryo diameter, the blastocyst can be modeled as a thin-walled

Table 1. Summary of embryonic microphysiology

Parameter	Mean	SD
Mean pressure	1,400 Pa	300 Pa
Maximum pressure	1,500 Pa	300 Pa
Mean volume	$6.6 \times 10^5 \mu\text{m}^3$	$1.8 \times 10^5 \mu\text{m}^3$
Rate of volume increase	$22 \mu\text{m}^3$	$12 \mu\text{m}^3$
Osmolyte flux	$10.1 \times 10^6 \text{ s}^{-1}$	$6.72 \times 10^6 \text{ s}^{-1}$
Na-K ATPase density	$1.7 \times 10^3/\text{cell}$	$1.2 \times 10^3/\text{cell}$
Water permeability	$1.50 \mu\text{m}^3 \cdot \text{Pa}^{-1} \cdot \text{s}^{-1}$	$1.01 \mu\text{m}^3 \cdot \text{Pa}^{-1} \cdot \text{s}^{-1}$
Zona pellucida stiffness	31.0 kPa	15.9 kPa
Zona pellucida thickness	4.3 μm	1.4 μm
Zona pellucida breaking stress	5.4 kPa	4.5 kPa

pressure vessel (Eqs. 4–9). The model also leads to the conclusion that there exists a critical pressure and radial expansion beyond which further expansion and shell thickness decrease occurs without increase in pressure. This is broadly analogous to a balloon bursting after it is inflated beyond the critical pressure. As such, the model demonstrates that zona pellucida rupture and embryo hatching is driven by volumetric expansion, not pressure generation, as embryos do not spontaneously hatch after reaching the peak pressure but require zona thickness to decrease further until breaking. All embryos analyzed here were similar to the initial stages of balloon inflation and did not increase their radius significantly beyond the point of maximum pressure.

The elastic balloon model can be used to calculate the shell material stiffness: if the shell increases in radius from R_0 to R when pressurized to P , the shell stiffness is $E = 3PR^7/2t_0(R^6 - R_0^6)$. It can also be used more generally, to model pressure in a radially expanding balloon (Fig. 3A), assuming initial shell thickness of 4.3 μm and 31.0-kPa Young's modulus. The stiffness value was selected by measuring a population of embryos used in the experiment (Fig. 3B). During these experiments, initial shell thickness was measured at the start of cavity formation at 3.25 days post coitum (dpc). Even though the elastic model relies on major

assumptions about the idealized material properties, the average value of 31.0 kPa agrees well with previously published reports using localized stiffness measurements by micropipette aspiration, 37 kPa (10); microtactile sensor, 22.3 kPa (27); and injection needles, 42.2 kPa (11).

The model also makes it possible to estimate that, given the mean rate of volume increase of 22 $\mu\text{m}^3/\text{s}$, it would take 16.4 h for an embryo of 40- μm radius to increase its radius to 72 μm at which point shell thickness would decrease to one-third of the original size, at which point the embryos would be expected to hatch. The timing coincides with developmental timescale. The decrease of zona pellucida thickness can be explained and modeled by embryo microphysiology (Table 1) and the elastic model. However, in practice we found the hatching process to be more complex, defined by two distinct modes of zona failure and being dependent also on matrix degrading enzymes, which we therefore investigated.

Embryo Hatching Probability. After the pressure buildup and volume increase, the ultimate result is embryo hatching. We identified two distinct types, which we termed “pinhole” (Fig. 3C and Movie S3) and “rupture” (Fig. 3D and Movie S4). The first type of

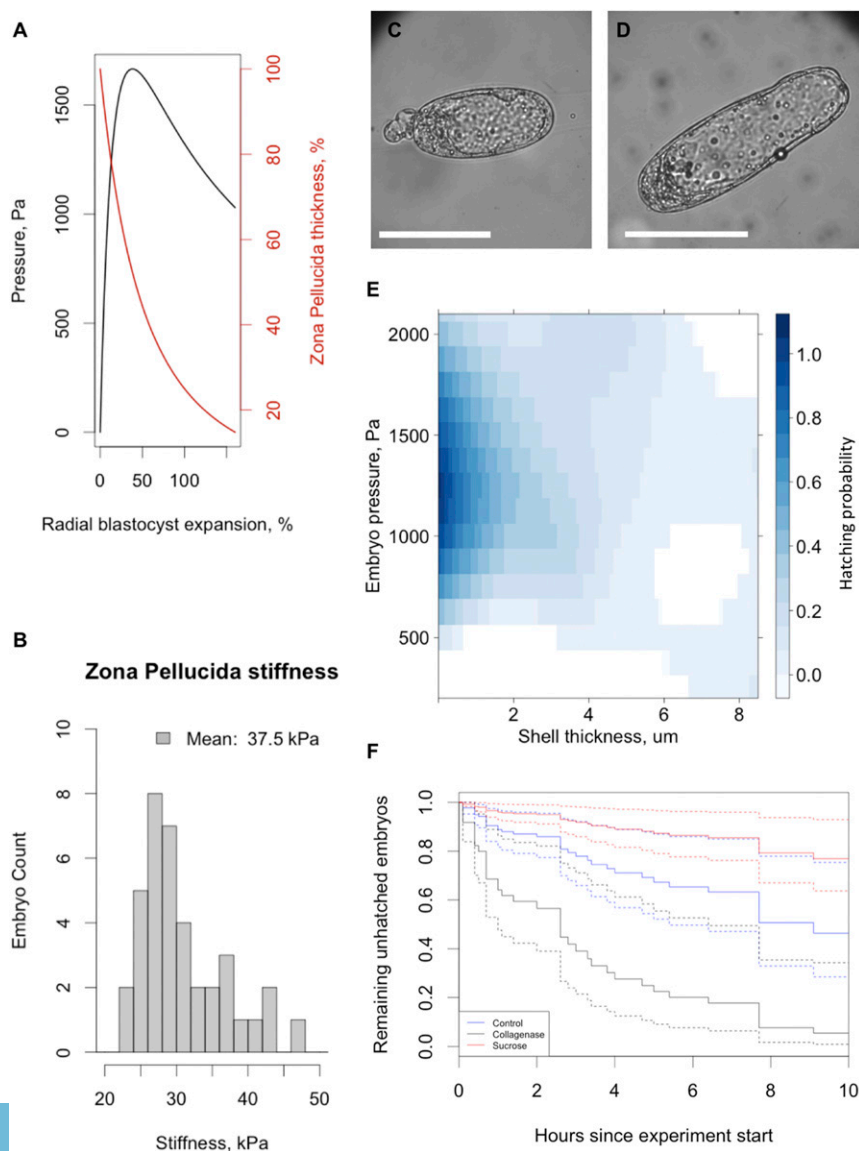


Fig. 3. Characterization of blastocyst hatching. (A) Pressure required to expand the embryo according to the thin-walled pressure vessel mathematical model. After an embryo reaches the maximum pressure at $\sim 50\%$ radial expansion, its further expansion does not require additional pressure. The model was calculated with stiffness of $E = 31.0$ kPa, mean shell thickness of $t = 4.3$ μm , and initial radius of $R_0 = 40$ μm , which are corresponding to median measured embryo values. (B) Measured zona pellucida stiffness during early development ($n = 38$). The stiffness was calculated from measured internal pressure, estimated equivalent sphere radius based on volume, and the mean starting radius and mean shell thickness. Eventual decrease in zona pellucida thickness leads to the hatching of an embryo, which may happen through a pinhole or rupture mechanism as depicted in C and D, respectively (Movies S3 and S4). (Scale bars: 100 μm .) (E) Measured probability of embryo hatching, as a function of embryo pressure and zona pellucida thickness. The probability map was constructed from shell thickness and pressure measurements, just before the hatching events. Hatching probability approached certainty as zona pellucida thickness decreased below 2.5 μm , as shown in a probability map. We found there to be a smaller dependence on blastocyst cavity pressure as soon as it increased over 500 Pa. However, the pressure and volumetric expansion did play a role in the hatching process as shown in the Cox survival model (F). Dashed lines indicate 95% confidence intervals; P value (from Cox regression model) for 150 mM sucrose treatment was 0.0209 and for 0.5 mg/mL collagenase treatment was 0.0014.

hatching could occur at relatively high zona pellucida thickness of over 3 μm and represented 45% of the total hatching events ($n = 19$ of 42). The remaining embryos (55%) hatched by rupturing the shell after its thickness decreased below 2.5 μm (Fig. 3E and *SI Appendix*, Fig. S4C), often after partially hatching through the pinhole mechanism. This process complicated data interpretation, as hatching events classified as pinhole would be converted into rupture depending on the developmental timeline. The overall hatching probability can be summarized as a function of embryo pressure and zona thickness measurements, which were taken and interpolated during hatching events (Fig. 3E). Despite embryo hatching probability approaching unity as zona thickness decreased, the embryos still required at least 0.5 kPa to hatch.

It has previously been shown that matrix degrading enzymes are important for shell breakage (20–22). To compare the relative contribution of mechanical forces and enzymatic digestion to hatching, we used media containing 0.5 mg/mL collagenase I to erode the zona pellucida and determined its effect on hatching probability. To test the role of pressure, we used 150 mM sucrose to lower the internal pressure. The experiment was fitted by the Cox survival model (Fig. 3F), and Kaplan–Meier statistic was then used to estimate the significance between treatment and control groups. Among the control group and sucrose-treated embryos, the likelihood coefficient was -1.075 , which meant that for any given point in time, sucrose-treated embryos were nearly three times less likely to hatch than controls (value of P of 0.021). Conversely, collagenase-treated embryos were 3.8 times more likely to hatch than controls (P value of 0.014).

Quantifying Microphysiology of Cryopreserved Embryos. The cryopreservation and thawing of preimplantation embryos is common during IVF, but little is known about what effect, if any, cryopreservation has upon blastocyst microphysiology and the pressure the blastocyst is able to generate. We therefore used our quantitative approach to look at how the cryopreservation/thawing process influences the embryo. We used three groups of mouse embryos, all from a C57BL/6J background: freshly flushed embryos at 2.5 dpc as controls and two groups of thawed embryos that had been cryopreserved at the 2.5 or 3.5 dpc stage. Cryopreserved embryos had been held in liquid nitrogen for at least 4 y. All embryos were cultured and measured at the stage equivalent to 3.5 dpc. We found no statistically significant differences between embryos thawed at stages 2.5 and 3.5 dpc. However, both thawed groups generated significantly lower pressure compared with freshly flushed embryos (Fig. 4A) (t test, P values < 0.05). This indicates that cryopreservation alters embryos in such a way that either their zona is less stiff, that is, “softer” (Fig. 4B and C), or that they are unable to develop the normal levels of volume growth required to generate pressure. To determine the consequences of reduced blastocyst pressure in cryopreserved embryos, we assessed hatching efficiency and found that hatching was delayed by ~ 10 h in comparison with noncryopreserved control embryos (*SI Appendix*, Fig. S4D). Taken together, our quantitative measurements of pressure reveal that cryopreservation alters mouse embryos in a previously unanticipated manner that has implications for hatching efficiency.

Conclusion

Mammalian embryo hatching is a biological process that is difficult to study quantitatively and model using existing approaches. We have developed a noninvasive technique to quantify embryo microphysiological parameters, which is useful not only for studying fundamental biological processes but also for evaluating embryo quality in assisted reproductive approaches. We applied this technique to developing mouse embryos, detailing microphysiological parameters as well as zona pellucida stiffness. Measuring these aspects of blastocyst development revealed the

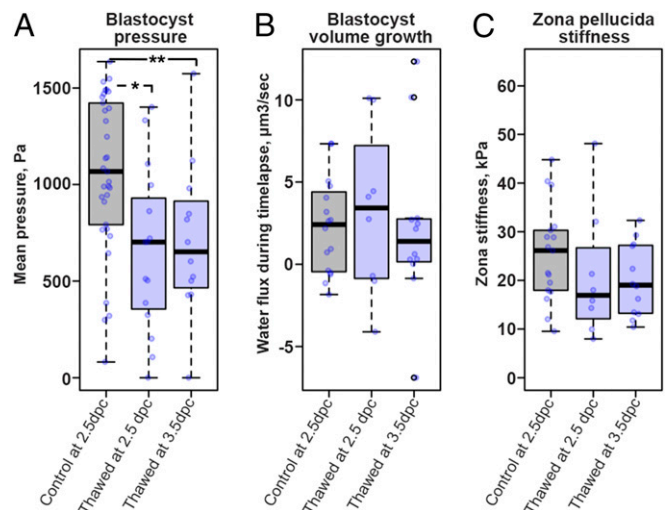


Fig. 4. Measuring the influence of cryopreservation on blastocyst pressure. Embryos cryopreserved at 2.5 dpc ($n = 15$) and 3.5 dpc ($n = 12$) were thawed and compared with embryos freshly flushed at 2.5 dpc ($n = 33$). All measurements were made at the equivalent of E3.5. (A) Cryopreserved embryos generate significantly lower pressure compared with freshly collected embryos. (B) Blastocyst volume growth is similar in the three groups. (C) Zona pellucida stiffness shows a trend toward being reduced in cryopreserved embryos. Calculations of volume growth and stiffness require time derivatives, which introduce more noise and dispersion, making statistical significance harder to establish despite large differences among the means. Outliers have been excluded for clarity in the plots in B and C. * $P < 0.05$ and ** $P < 0.01$, pairwise t test.

magnitude of hydraulic pressures inside blastocysts and allowed us to develop a mathematical model based on inflating a thin-shell pressure vessel. Using this framework, we showed that hatching is limited by the rate of ion transport, which ultimately draws in water, increases embryo volume, and thereby reduces zona thickness. By experimentally altering blastocyst pressure, we were able to investigate how hatching dynamics are defined by both physiology and mechanical properties of the zona.

We used our approach to study the effect of cryopreservation on blastocysts and found that thawed embryos generated a significantly lower pressure compared with fresh embryos, accompanied by a considerable delay in hatching. Hatching is a prerequisite to implantation and continued development of the conceptus. Assisted reproductive approaches increasingly utilize cryopreservation, highlighting the importance of evaluating in quantitative detail its effect not only on hatching, but other aspects of embryo microphysiology. We focused on the mouse model due to its long-standing importance in *in vitro* studies. Other mammalian species may have different embryo microphysiology and zona pellucida properties, and it will be interesting to uncover what differences, if any, exist. Finally, our method is broadly applicable for characterizing pressurized cavities in other contexts, such as stem cell-derived organoids or cysts.

Materials and Methods

Preparing Cylindrical Hydrogels. Hydrogels with cylindrical cavities were prepared by casting polyacrylamide gels around small-diameter wire (40 μm). Acrylamide/bisacrylamide (37.5:1) mixture was used (5.0% by mass), which corresponded to 4.2-kPa stiffness. Ammonium persulfate (0.1%) and tetramethylethylenediamine (1%) were added to polymerize polyacrylamide. The wire was removed, forming cylindrical cavities, and the hydrogels equilibrated in embryo culture medium by changing the solution three times in 1 h. Embryos were then inserted into the channels using a glass capillary having a diameter slightly larger than the embryo, which was used to stretch

open the hydrogel channel before injecting the embryos and letting the channels relax and deform the embryos.

Imaging Setup and Image Analysis. Imaging was performed on a Zeiss Axiovert spinning-disk confocal microscope equipped with a Hamamatsu emCCD camera and a 37 °C and 5% CO₂ incubator. Embryos were cultured for periods of 2 h between 3.0 and 4.0 dpc stages, recording images every 6 min. Embryos were analyzed using a combination of manual and automatic image analysis approaches. Manual analysis was used to ensure no algorithmic bias, while the high-throughput analysis relied on computational methods. The main measured parameters were channel diameter and embryo width and length, which made it possible to calculate micropophysiological embryo properties. Zona thickness was measured only manually, at either of the unconfined embryo ends. Blastocyst cavity volume was determined from the total embryo volume by subtracting a constant volume of the inner cell mass cells assumed to be $2.1 \times 10^{-5} \text{ um}^3$. Average volumes and pressures were calculated by taking mean values of an embryo's time lapse, summarizing them, and taking means of the means (data seen in histograms in Fig. 2).

Thin-Walled Vessel Pressure Derivation. As is familiar to anyone who has inflated a party balloon, the inflation is difficult at first, but once the balloon is modestly inflated, it becomes much easier. This occurs because the pressure in the balloon first increases with inflation, and then, past a critical volume, the pressure in the balloon falls. This "balloon instability" ultimately has a geometric origin: As the balloon inflates, its walls become thinner and flatter and thus able to contain less pressure. We can understand this phenomenon (28) by considering a spherical rubber balloon, with natural radius R_0 and thickness t . If the balloon is inflated such that its radius dilates to $R = \lambda R_0$, then circumferences of the balloon dilate by λ , while to conserve volume of the rubber, the thickness of the balloon must fall to t/λ^2 . Therefore, the deformation gradient in the rubber will be as follows:

$$F = \begin{pmatrix} \lambda & 0 & 0 \\ 0 & \lambda & 0 \\ 0 & 0 & 1/\lambda^2 \end{pmatrix}, \quad [4]$$

and assuming the rubber is well described by a neo-Hookean energy, the total elastic energy will be as follows:

- Hammadeh ME, Fischer-Hammadeh C, Ali KR (2011) Assisted hatching in assisted reproduction: A state of the art. *J Assist Reprod Genet* 28:119–128.
- Aplin JD (2006) Embryo implantation: The molecular mechanism remains elusive. *Reprod Biomed Online* 13:833–839.
- Jun SH, Milki AA (2004) Assisted hatching is associated with a higher ectopic pregnancy rate. *Fertil Steril* 81:1701–1703.
- Diedrich K, Fauser BCJM, Devroey P, Griesinger G; Evian Annual Reproduction (EVAR) Workshop Group (2007) The role of the endometrium and embryo in human implantation. *Hum Reprod Update* 13:365–377.
- Gabrielsen A, Fedder J, Agerholm I (2006) Parameters predicting the implantation rate of thawed IVF/ICSI embryos: A retrospective study. *Reprod Biomed Online* 12: 70–76.
- Campàs O, et al. (2014) Quantifying cell-generated mechanical forces within living embryonic tissues. *Nat Methods* 11:183–189.
- du Roure O, et al. (2005) Force mapping in epithelial cell migration. *Proc Natl Acad Sci USA* 102:2390–2395, and erratum (2005) 102:14122.
- Li M, et al. (2013) Investigating the morphology and mechanical properties of blastomeres with atomic force microscopy. *Surf Interface Anal* 45:1193–1196.
- Papi M, et al. (2010) Mechanical properties of zona pellucida hardening. *Eur Biophys J* 39:987–992.
- Khalilian M, Navidbakhsh M, Valojerdi MR, Chizari M, Yazdi PE (2010) Estimating Young's modulus of zona pellucida by micropipette aspiration in combination with theoretical models of ovum. *J R Soc Interface* 7:687–694.
- Sun Y, Wan KT, Roberts KP, Bischof JC, Nelson BJ (2003) Mechanical property characterization of mouse zona pellucida. *IEEE Trans Nanobioscience* 2:279–286.
- Murayama Y, Constantinou CE, Omata S (2004) Micro-mechanical sensing platform for the characterization of the elastic properties of the ovum via uniaxial measurement. *J Biomech* 37:67–72.
- Hirate Y, et al. (2013) Polarity-dependent distribution of angiominin localizes Hippo signaling in preimplantation embryos. *Curr Biol* 23:1181–1194.
- Plusa B, et al. (2005) Downregulation of Par3 and aPKC function directs cells towards the ICM in the preimplantation mouse embryo. *J Cell Sci* 118:505–515.

$$W_{\text{tot}} = \frac{E}{6} (Tr(F \cdot F^T) - 3) 4\pi R_0^2 t = \frac{E}{6} \left(2\lambda^2 + \frac{1}{\lambda^4} - 3 \right) 4\pi R_0^2 t. \quad [5]$$

Since in this inflation the volume of the balloon changes from its undeformed volume V_0 to $V = \lambda^3 V_0$, we can express this elastic energy as follows:

$$W_{\text{tot}} = \frac{E}{6} \left(2 \left(\frac{V}{V_0} \right)^{\frac{2}{3}} + \left(\frac{V}{V_0} \right)^{-\frac{4}{3}} - 3 \right) 4\pi R_0^2 t, \quad [6]$$

and we can calculate the pressure in the balloon as follows:

$$P = \frac{\partial W_{\text{tot}}}{\partial V} = \frac{E}{6} \left(\frac{4}{3} \left(\frac{V}{V_0} \right)^{-\frac{1}{3}} - \frac{4}{3} \left(\frac{V}{V_0} \right)^{-\frac{7}{3}} \right) \frac{4\pi R_0^2 t}{V_0}. \quad [7]$$

This pressure can be recast in terms of R and R_0 as follows:

$$P = \frac{\partial W_{\text{tot}}}{\partial V} = \frac{2Et}{3R_0} \left(\left(\frac{R}{R_0} \right)^{-1} - \left(\frac{R}{R_0} \right)^{-7} \right). \quad [8]$$

This form for the pressure does indeed rise from zero for modest inflations (R a little above R_0), but then reaches a maximum pressure when

$$\frac{\partial P}{\partial R} = \frac{2Et}{3R_0} \left(-\left(\frac{R}{R_0} \right)^{-2} + 7 \left(\frac{R}{R_0} \right)^{-8} \right) = 0, \quad [9]$$

which occurs when $R = 7^{1/6} R_0 \sim 1.38 R_0$, and the pressure falls with subsequent additional inflation. The form of pressure-inflation curve is shown in Fig. 3A, the essential point being that if the embryo can exert enough pressure to inflate the zona (balloon) radius by 38%, then it does not require additional pressure to expand the shell further until it breaks. The exact value of 38% is particular to the neo-Hookean rubber model, but calculations for other material models, and experiments with real balloons, indicate that the critical dilation reliably lies between $7^{1/6}$ and 1.5 (29). Also, for thin-walled cylindrical pressure vessels, the longitudinal stress can be expressed as a combination of pressure, wall thickness, and the radius of the spherical part: $\rho = Pr/2t$, which makes it possible to estimate the mean breaking stress of the zona pellucida.

ACKNOWLEDGMENTS. This work was supported by a studentship (to K.L.) from the Biotechnology and Biological Sciences Research Council (BB/J014427/1), Lithuanian Science Council Postdoctoral Award (code 09.3.3-LMT-K-712-02-0067), the Wellcome Trust (203141/Z/16/Z), and a Wellcome Senior Investigator Award (103788/Z/14/Z) (to S.S.).

- Watson AJ, Natale DR, Barcroft LC (2004) Molecular regulation of blastocyst formation. *Anim Reprod Sci* 82–83:583–592.
- Eckert JJ, Fleming TP (2008) Tight junction biogenesis during early development. *Biochim Biophys Acta* 1778:717–728.
- Moriwaki K, Tsukita S, Furuse M (2007) Tight junctions containing claudin 4 and 6 are essential for blastocyst formation in preimplantation mouse embryos. *Dev Biol* 312: 509–522.
- Barcroft LC, Offenberg H, Thomsen P, Watson AJ (2003) Aquaporin proteins in murine trophoctoderm mediate transepithelial water movements during cavitation. *Dev Biol* 256:342–354.
- Edashige K, Sakamoto M, Kasai M (2000) Expression of mRNAs of the aquaporin family in mouse oocytes and embryos. *Cryobiology* 40:171–175.
- Thomas M, Jain S, Kumar GP, Laloraya M (1997) A programmed oxyradical burst causes hatching of mouse blastocysts. *J Cell Sci* 110:1597–1602.
- Perona RM, Wassarman PM (1986) Mouse blastocysts hatch in vitro by using a trypsin-like proteinase associated with cells of mural trophoctoderm. *Dev Biol* 114:42–52.
- Sawada H, Yamazaki K, Hoshii M (1990) Trypsin-like hatching protease from mouse embryos: Evidence for the presence in culture medium and its enzymatic properties. *J Exp Zool* 254:83–87.
- Biggers JD, Bell JE, Benos DJ (1988) Mammalian blastocyst: Transport functions in a developing epithelium. *Am J Physiol* 255:C419–C432.
- Boardman LJ, Lamb JF, McCall D (1972) Uptake of [³H]ouabain and Na pump turnover rates in cells cultured in ouabain. *J Physiol* 225:619–635.
- Pollack LR, Tate EH, Cook JS (1981) Turnover and regulation of Na-K-ATPase in HeLa cells. *Am J Physiol* 241:C173–C183.
- El Mernissi G, Doucet A (1984) Quantitation of [³H]ouabain binding and turnover of Na-K-ATPase along the rabbit nephron. *Am J Physiol* 247:F158–F167.
- Murayama Y, et al. (2006) Mouse zona pellucida dynamically changes its elasticity during oocyte maturation, fertilization and early embryo development. *Hum Cell* 19: 119–125.
- Müller I, Strehlow P (2004) *Rubber and Rubber Balloons: Paradigms of Thermodynamics*. Lecture Notes in Physics, eds Müller I, Strehlow P (Springer, Heidelberg).
- Gent AN (2005) Elastic instabilities in rubber. *Int J Non Linear Mech* 40:165–175.